Analysis of Rotorcraft Dynamics by Bred Vector

Ivana Y. Sumida[a] [b1], Thiago G. Ritto [c] and Haroldo F. de Campos Velho[d]

[a]Applied Computing Graduate Program - National Institute for Space Research, São José dos Campos, SP, Brazil

[b]Flight Test Research Institute - Aerospace Technology and Science Department, São José dos Campos, SP, Brazil

[c]Department of Mechanical Engineering - Federal University of Rio de Janeiro, Rio de Janeiro, RJ, Brazil

[d]Associated Laboratory for Computing and Applied Mathematics - National Institute for Space Research, São José dos Campos, SP, Brazil

Received on January 01, 2015 / accepted on *****, 2015

Abstract

The rotorcraft dynamic behavior is very important issue. Such simulation can be used identify many real- world situations, such as ground resonance. The latter phenomenon can lead to the total destruction of the rotorcraft. It is usually occurring during helicopter landing, take-off and ground manoeuvres, and is caused by the interaction between the flow air from the main rotor blades and the fuselage structure. The prediction of this behavior is usually very difficult, mainly in cases which the rotorcraft parameters are obtained by measurement instruments, frequently subject to acquisition errors.

Simulation of dynamical phenomena is a fundamental tool nowadays. The study to identify zones, or time periods, where the simulation can give a good or bad representation of the dynamical process is named predictability.

In this paper, the predictability of the rotorcraft dynamic behavior can be formulated as a classification problem. Bred vector is the difference between a reference dynamics and a perturbed dynamics, after some time-steps. The procedure is applied on a ground resonance simulation.

Keywords: Ground resonance, bred vector.

1. Helicopter Dynamics Characterization

Helicopters are highly nonlinear apparatus and it is interesting investigate how the variety of nonlinearities can affect their behavior. One phenomenon clearly nonlinear is a particular mode of helicopter vibration known

[1]E-mail Corresponding Author: ivanayoshie@yahoo.com.br

as ground resonance. This phenomenon may occur over a range of rotor speed, and it is attributed to the coupling of lead-lag frequency of the rotor blades to natural frequencies of the dynamic system constructed together with fuselage and landing gears [1]. It has been observed since the inception of helicopter development, and several helicopters and autogyros have been destroyed or badly damaged as a result of its effects, as you can see in Figure 1.

Figure 1: Ground Resonance [7]

The pioneer work on ground resonance was done by [2]. Some other contributions were made by lee who propose a method to predict the vibration and unstable range of rotor speed, including the nonlinear characteristics in the landing gear and [3, 4] studies both air and ground resonance. Furthermore, [5] analysis a rotor helicopter on the basis of a set of nonlinear differential equations taking into account the forces and moments produced by landing gear.

2. Dynamical Model Equations

A three-blade helicopter is modeled by a simplified multibody system. The basic hypotheses are the following ones: (1) the movement occurs only in (x, y) plane, (2) the blades are rigid bars, (3) the rotor head is a rigid cylinder with constant rotational speed, and (4) only the first axial/lateral modes of the helicopter are taken into account. With such hypotheses, the system has five degrees of freedom (DOF): the x and y displacements of the center of mass of the rotor head, and the blade angles β_i ($i = 1, ..., N$), where N is the number of blades, which is three in the present model. Using the mathematical model developed by the authors [6], Figure 2 shows the general scheme of the proposed model.

The blades are attached to the rotor head through a point called link, distant d from origin O, the geometric center of the rotor head. At each link, there is a linear torsional spring and damping.

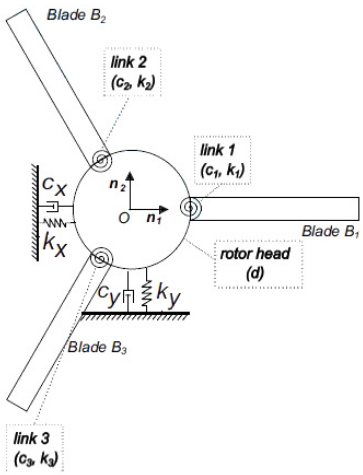

Figure 2: System Coordinate and Degrees of Freedom [6]

Let us consider a inertial frame of reference, with basis $\{\mathbf{n}_1, \mathbf{n}_2\}$, and a Cartesian coordinate system with origin O. The position of the center of mass of the rotor head H^* with respect to the origin can be written as:

$$O\mathbf{r}H^*(t) = [x(t) + e\cos(\epsilon + \Omega t)]\mathbf{n}_1 + [y(t) + e\sin(\epsilon + \Omega t)]\mathbf{n}_2 \tag{1}$$

where x is the displacement of the geometric center of the rotor head in the direction of $\mathbf{n}_1$, y is the displacement of the geometric center of the rotor head in the direction of $\mathbf{n}_2$, Ω is the rotor head constant rotation speed, e is the eccentricity of the rotor head, ϵ is the angle of the eccentricity (figure 3).

Considering that each blade has a phase angle (ϕ_i), or azimuth, the position of the center of mass of the blade B_i with respect to O can be written as:

$$\begin{aligned} O\mathbf{r}B_i(t) = &[x(t) + d\cos(\phi + \Omega t) + \left(\frac{hB_i}{2}\right)\cos(\phi + \Omega t + \beta_i(t))]\mathbf{n}_1 \\ &+[y(t) + d\sin(\phi + \Omega t) + \left(\frac{hB_i}{2}\right)\sin(\phi + \Omega t + \beta_i(t))]\mathbf{n}_2 \end{aligned} \tag{2}$$

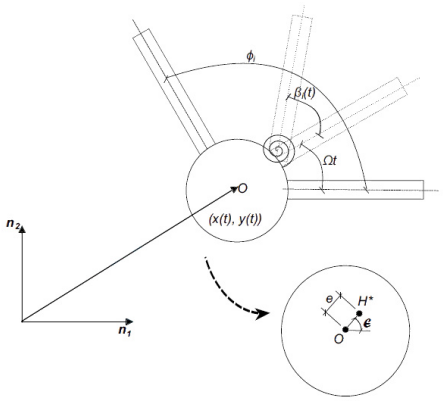

Figure 3: Blade Dynamics Scheme [6]

where h_{B_i} is the length of the i-th blade and β_i is the angle of the i-th blade in the direction of $\mathbf{n}_3$ with respect to a frame that rotates with the rotor head.

2.1 Newton Second Law

Applying Newton's second law (figure 4), we have:

$$\mathbf{F} = \frac{d\mathbf{G}^T}{dt} \tag{3}$$

where $\mathbf{G}^T$ is the total linear momentum of the system and the derivative is with respect to the inertial frame of reference. The vector with external forces $\mathbf{F}$ acting on the system due to the tower stiffness/damping and due to gravity are written as:

$$\mathbf{F} = [-c_x\dot{x}(t) - k_x x(t)]\mathbf{n}_1 + [-c_y\dot{y}(t) - k_y y(t) - (Nm_{B_i} + m_H)g]\mathbf{n}_2 \tag{4}$$

where g is the acceleration of gravity, k_x, k_y, c_x, c_y are the stiffness and damping coefficients related to the helicopter, in the $\mathbf{n}_1$ and $\mathbf{n}_2$ directions. The i-th blade mass is m_{B_i} , and m_H is the sum of the mass of the rotor head.

The total linear momentum is composed by the linear momentum of the rotor head plus the linear momentum of the blades. The linear momentum of the nacelle/tower is given by:

$$\mathbf{G}_H = m_H\mathbf{v}_H* \tag{5}$$

where $\mathbf{v}_{H}*$ is the velocity of the center of mass of the rotor head, which is the derivative of the position $O_{H}*$ with respect to the inertial frame of reference. The linear momentum of the i-th blade is given by:

$$\mathbf{G}_{B_i} = m_{B_i}\mathbf{v}_{B_i} \tag{6}$$

where $\mathbf{v}_{B_i}$ is the velocity of the center of mass of the i-th blade, which is the derivative of the position $O\mathbf{r}B_i$ with respect to the inertial frame of reference. The total linear momentum of the system, if all blades have the same mass, is then defined by:

$$\mathbf{G}_T = \mathbf{G}_H + \sum_{n=1}^{N}\mathbf{G}_{B_i} = m_H\mathbf{v}_H * + m_B\sum_{n=1}^{N}\mathbf{v}_{B_i} \tag{7}$$

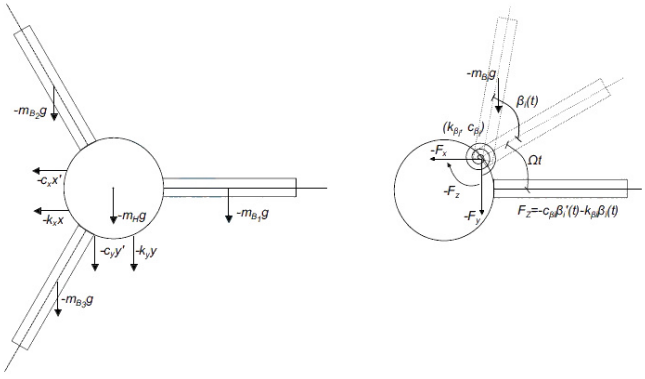

Figure 4: Acting Forces [6]

After some manipulations, we get the first two equations of motion of the system:

$$\begin{aligned}(Nm_B + m_H)\ddot{x}(t) + c_x\dot{x}(t) + k_x x(t) = em_H\Omega^2\cos(\epsilon + \Omega t) + \\ dm_B\Omega^2\sum_{n=1}^{N}\cos(\phi_i + \Omega t) + m_B\left(\frac{h_B}{2}\right)\sum_{n=1}^{N}[\ddot{\beta}_i(t)\sin(\phi_i + \Omega t + \beta_i(t)) + \\ (\Omega + \dot{\beta}_i(t))^2\cos(\phi_i + \Omega t + \beta_i(t))]\end{aligned} \tag{8}$$

$$
\begin{aligned}
(Nm_B + m_H)\ddot{y}(t) + c_y\dot{y}(t) + k_y y(t) + (NmB_i + m_H)g = \\
em_H\Omega^2 \sin(\epsilon + \Omega t) + dm_B\Omega^2 \sum_{n=1}^{N} \sin(\phi_i + \Omega t) + \\
m_B \left(\frac{h_B}{2}\right) \sum_{n=1}^{N} [-\ddot{\beta}_i(t) \cos(\phi_i + \Omega t + \beta_i(t)) + \\
(\Omega + \dot{\beta}_i(t))^2 \sin(\phi_i + \Omega t + \beta_i(t))]
\end{aligned} \tag{9}
$$

where the over dot is the derivative with respect to time.

Unfortunately, these equations are not sufficient to analyze the system because the system has $(N + 2)$ DOFs. One possibility is to develop three equations of motion for each rigid body, and end up with $3(N + 2)$ equations; but, fortunately, we do not need so many equations. Since we are not interested in the interaction forces among the rigid bodies, we will calculate the angular momentum with respect to each link, so that only N more equations are required to analyze the system. The price to pay is that the link is a moving point not coincident with the center of mass, therefore, attention is required because $\mathbf{M} \neq d\mathbf{H}/dt$.

2.2 Euler Law

Applying the Euler's law, we have:

$$
\mathbf{M}_{L_i}^{B_i} = \frac{d\mathbf{I}_{L_i}^{B_i}\omega}{dt} + (m_{B_i}) L_i\mathbf{r}B_i{}^* \times \mathbf{a}L_i \tag{10}
$$

where $\mathbf{M}_{L_i}^{B_i}$ is the vector of external moments acting on the i-th blade with respect to link L_i. The angular inertia tensor of the i-th blade with respect to link L_i is $\mathbf{I}_{L_i}^{B_i}$, $L_i\mathbf{r}B_i$ is the position of the center of mass of the i-th blade with respect to L_i , and $\mathbf{a}L_i$ is the acceleration of L_i. Note that the additional term on the right of the above equation appears because the point L_i has an acceleration which is not zero. The vector of external moments acting on the i-blade is given by:

$$
\mathbf{M}_{L_i}^{B_i} = [-c_i\dot{\beta}_i(t) - k_i\beta_i(t) - m_{B_i} g \left(\frac{h_{B_i}}{2}\right) \cos(\phi_i + \Omega(t) + \beta_i(t)]\mathbf{b}_3 \tag{11}
$$

where k_i and c_i are i-th blade stiffness and damping coefficients. The position of the center of mass of the i-th blade with respect to L_i can be written as:

$$L_i rB_i(t) = \left[\left(\frac{h_{B_i}}{2}\right)\cos(\phi_i + \Omega(t) + \beta_i(t)\right]\mathbf{n}_1 + \left[\left(\frac{h_{B_i}}{2}\right)\sin(\phi_i + \Omega(t) + \beta_i(t)\right]\mathbf{n}_2 \tag{12}$$

and the acceleration of the link is given by:

$$\mathbf{a}_{L_i}(t) = [\ddot{x}(t) - d\Omega^2\cos(\phi_i + \Omega(t)]\mathbf{n}_1 + [\ddot{y}(t) - d\Omega^2\sin(\phi_i + \Omega(t)]\mathbf{n}_2\ . \tag{13}$$

Again, after some manipulations, we get the extra N equations of motion of the system ($i = 1, ..., N$):

$$\frac{1}{3}mB_i h_{B_i}^2\ddot{\beta}_i(t) + c_i\dot{\beta}_i(t) + k_i\beta_i(t) + mB_i\frac{hB_i}{2}d\Omega^2\sin\beta_i + mB_i g\frac{hB_i}{2}\cos(\phi_i + \Omega t + \beta_i(t)) = mB_i\frac{hB_i}{2}[\ddot{x}(t)\sin(\phi_i + \Omega t + \beta_i(t)) - \ddot{y}(t)\cos(\phi_i + \Omega t + \beta_i(t))] \tag{14}$$

Setting $N = 3$ (three blade system), the five equations of motion of the proposed model are given by Eqs. (8), (9) and (14), which form a set of coupled, nonlinear, second order ordinary differential equations, that must be solved numerically.

3. Bred Vector Approach

The bred vector approach was developed by Toth and Kalnay [8, 9]. It has been used in the American National Center for Environmental Prediction (NCEP) to evaluate the prediction, and it was also employed in several nonlinear models [10, 13, 14, 15].

In this methodology, the bred vectors are found out dynamically from the nonlinear model which is executed twice. First of all, the model is run with the original data (control run) next another execution is realized with a small perturbation added to it. After a fixed number of time steps, the difference between these two executions is the bred vector. A measure of the

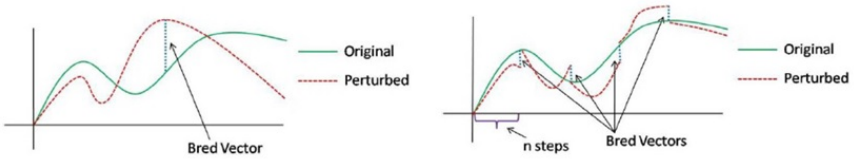

Figure 5: Bred vector growth [16]

flow instability could be computed from the growth rate of the bred vectors [9, 13]. Figure 5 illustrates bred vectors growth.

The bred vector algorithm [11] is described in detail below:

1. Start with a initial perturbation $\delta r_0 = r_0 + \delta r_0$. The initialization is executed only once

2. Add the perturbation calculated in the previous step to the basic solution, integrate the perturbed condition with the nonlinear model for a fixed number of time steps, and subtract the original unperturbed solution from the perturbed nonlinear integration $\delta r_0(t) = \Phi(\delta r_0 + r_0, t_0 + n\Delta t) - \Phi(r_0, t_0 + n\Delta t)$

3. Evalute the growth ratio $g = \frac{1}{n} \ln \left(\frac{\|\delta r(t)\|}{\|\delta r_0\|} \right)$

4. Re-scale the perturbation, and repete the process.

Bred vectors have been used with success to predict the behavior of chaotic systems such as the Lorenz strange attractor ref and the three-waves systems ref. Our objective is to extend such methodology to investigate the predictability for the helicopter dynamical system, with focus on critical behaviour: the ground resonance phenomenon.

4. Results

Computer tests were conducted in an Intel Core I5 2.27 GHz under Linux operating system. Our mathematical model was implemented in Matlab R2011b. For executing the dynamical system, the following parameters were assumed: $k_x = k_y = 113$ lb/ft, $m_{B_i} = 0.1$ slug, $m_H = 6.8$ slugs, $\Omega = 90$ rad/s, and $h_B = 10$ ft. The time integration for the equation system was the fourth-order RungeKutta scheme with a time-step $\Delta t = 10^{-3}$. Figure 6 illustrates the trajectory generated, representing the movement of the rotor head, and the dynamics is confined in a bounded region.

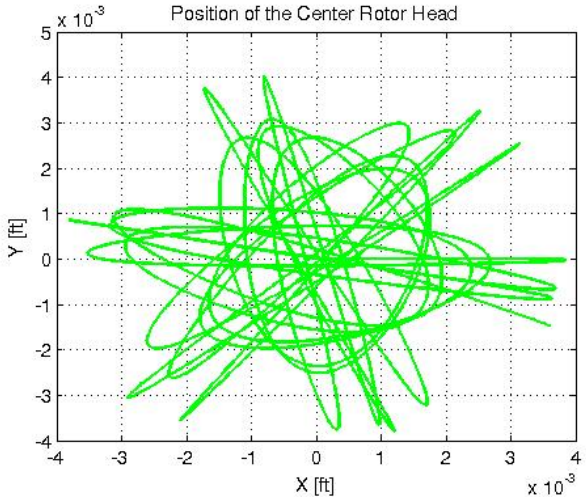

Figure 6: Position of the Center Rotor Head

In our study, the dynamics was separated into two regimes. One regime is identified "turn right" Figure 7(a), and the other regime "turn left", Figure 7(b). Similar idea was applied in [10], where the Lorenz system was identifed embracing two different regimes – the authors named as two *seasons* (e.g."warm" and "summer"). The Lorenz system is low dimension one, but is hard to evaluate when a regime will change and how long it will return.

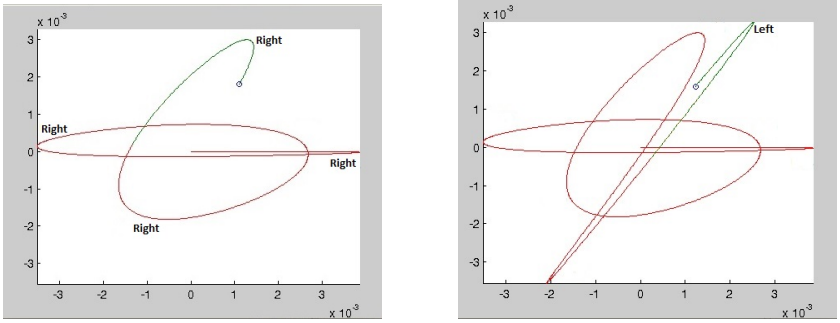

(a) Right Regime (b) Left Regime

Figure 7: Right and Left Regime

The breeding was performed on two executions. The first run is called *control*. The second run started from an initial perturbation δx_0 added

to the control at time t_0. The difference δx between the perturbed and the control run was taken at every 8 times steps. The growth rate of the perturbation was measured per time step as [10]:

$$g = \frac{1}{n} \ln \left(\frac{\|\delta x\|}{\|\delta x_0\|} \right) . \tag{15}$$

Figure 8 shows the bred vector after 8 times steps. We used 5 colors to indicate the bred vector growth intervals, described below:

1. yellow star: $g \in [-0.0930, -0.0343[$
2. green star: $g \in [-0.0343, 0.0244[$
3. blue star: $g \in [0.0244, 0.0832[$
4. red star: $g \in [0.0832, 0.01419[$
5. black star: $g >= 0.01419$

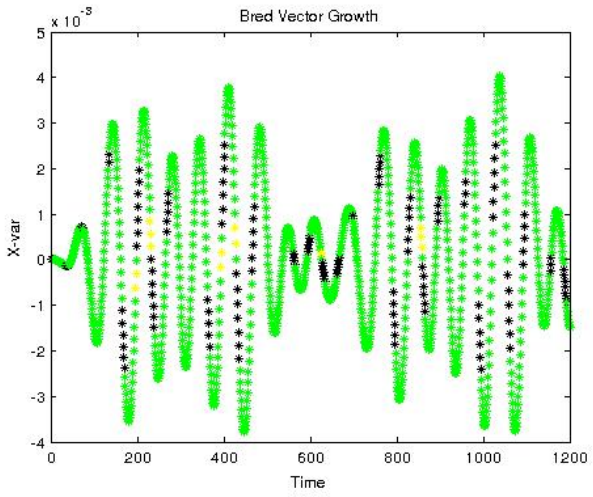

Figure 8: X(t) for Ground Resonance Model Colored with the Bred Vector Intervals.

From the observation of the system depicted in Figures 7(a), 7(b) and 8 the following rules can be expressed:

1. The trajectory turn right or turn left, on average, after at each 29 stars.

2. After a period of time appears a dynamical pattern in the trajectory: turn right five times, one time left and five times right again and two times left. At the first turn right five times appears a set sequence of approximately two yellow, one green and seven black stars

For future work, we will describe the dynamics as a classification problem, mapping a type of dynamics in different classes. The magnitude of bred vector is the input for a neuro-fuzzy classifier [12]. The bred vector methodology will be used to generate pairs of input/output required for Neuro-Fuzzy system ANFIS (Adaptive Neuro Fuzzy Inference System), employed as a classifier. Formulating the problem as a *dynamical classes* is a procedure to address the predictabilty of the dynamical system.

References

[1] Lee, Y.K. and Kim, K.J. Ground resonance analysis for an eight-degrees-of-freedom rotorcraft with double-stage oleo-pneumatic shock absorbers, Journal of a Aircraft, Vol 47, No. 5, pp. 65-91, 2010.

[2] Coleman, R.P. and Feingold, A.M. Theory of self-excited mechanical oscillations of helicopter rotors with hinged blades, NACA Report 1351, 1958.

[3] Lytwyn, R., Miao ,W. and Woitsch, W. Airborne and ground resonance of hingeless rotors, Journal of the American Helicopter Society, Vol 17, No. 2, pp. 2-9, 1972.

[4] Jang, J. and Chopra, I. Ground air resonance of a bearingless rotors in hover, 28^{th} Structures, Structural Dynamics and Materials Conference. Monterey, CA, U.S.A., 1987.

[5] Dzygadlo, Z. and Kowaleczko, G. Ground resonance of a helicopter, Journal of Theoretical and Applied Mechanics, Vol 1, No. 38, pp. 65-91, 2000.

[6] Gonzaga, F.G. Modelos computacionais para análise da vibração acoplada rotor-pás com aplicação em turbinas eólicas e ressonância de solo de helicópteros, Projeto de Graduação, Departamento de Engenharia Mecânica da Escola Politécnica, Universidade Federal do Rio de Janeiro, 2013.

[7] Garrison, P. How things work: ground resonance, http://www.airspacemag.com/flight-today/how-things-work-ground-resonance-94660854/?no-ist, Access in 09/20/2016, 2008.

[8] Toth, Z. and Kalnay, E. Ensemble forecasting at NCEP: the generation of perturbations, Bull. Amer. Meteor. Soc., Vol 74, pp. 2317-2330, 1993.

[9] Toth, Z. and Kalnay, E. Ensemble forecasting at NCEP and the breeding method, Monthly Weather Review, Vol 126, 1997.

[10] Evans, E., Bathi, N.K., Kinney, J., Peña, L.P.M., Yang, S-C, Kalnay, E. and Hansen, J. Rise undergraduates find that regime changes in Lorenz's model are predictable, Bull. Amer. Meteor. Soc., Vol 85, pp. 520-524, 2004.

[11] Kalnay, E. Atmospheric modeling, data assimilation and predictability, Chapter 6. Cambridge University Press, 2001.

[12] Santos, P.L.B., Sandri, S.A. and Campos Velho, H.F. Uncertainties formulated as a classification problem applied to chaotic system, Mecánica Computacional, Vol 33, pp. 1783-1791, 2014.

[13] Cintra, R.S.C. and Campos Velho, H.F. Predictability for a chaotic solar plasma system,Iberian and LatinAmerican Congress on Computational Methods for Engineering (XXIX CILAMCE), pp. 1-8, 2008.

[14] Pasini, A. and Pelino, V. Can we estimate atmospheric predictability by performance of neural network forecasting? The toy case studies of unforced and forced Lorenz models, CIMSA 2005 - IEEE International Conference on Computational Intelligence for Measurement Systems and Applications, 2005.

[15] Wang, X. and Bishop, C.H. A comparison of breeding and ensemble transform Kalman filter ensemble forecast schemes, Jounal of the Atmospheric Sciences, Vol 60, No. 9., 2003.

[16] Santos, P.L.B. Previsibilidade em sistemas caóticos utilizando sistemas neuro-difusos, Dissertação de Mestrado, Instituto Nacional de Pesquisas Espaciais (INPE), São José dos Campos. Annuals of the New York Academy of Science, 357, 422-434, 2014.